Climatology Models for Extreme Hurricane Winds near the United States

THOMAS H. JAGGER AND JAMES B. ELSNER

Department of Geography, The Florida State University, Tallahassee, Florida

(Manuscript received 12 August 2005, in final form 13 December 2005)

ABSTRACT

The rarity of severe coastal hurricanes implies that empirical estimates of extreme wind speed return levels will be unreliable. Here climatology models derived from extreme value theory are estimated using data from the best-track [Hurricane Database (HURDAT)] record. The occurrence of a hurricane above a specified threshold intensity level is assumed to follow a Poisson distribution, and the distribution of the maximum wind is assumed to follow a generalized Pareto distribution. The likelihood function is the product of the generalized Pareto probabilities for each wind speed estimate. A geographic region encompassing the entire U.S. coast vulnerable to Atlantic hurricanes is of primary interest, but the Gulf Coast, Florida, and the East Coast regions are also considered. Model parameters are first estimated using a maximum likelihood (ML) procedure. Results estimate the 100-yr return level for the entire coast at 157 kt ($\pm$10 kt), but at 117 kt ($\pm$4 kt) for the East Coast region (1 kt = 0.514 m s^{-1}). Highest wind speed return levels are noted along the Gulf Coast from Texas to Alabama. The study also examines how the extreme wind return levels change depending on climate conditions including El Niño–Southern Oscillation, the Atlantic Multidecadal Oscillation, the North Atlantic Oscillation, and global temperature. The mean 5-yr return level during La Niña (El Niño) conditions is 125 (116) kt, but is 140 (164) kt for the 100-yr return level. This indicates that La Niña years are the most active for the occurrence of strong hurricanes, but that extreme hurricanes are more likely during El Niño years. Although El Niño inhibits hurricane formation in part through wind shear, the accompanying cooler lower stratosphere appears to increase the potential intensity of hurricanes that do form. To take advantage of older, less reliable data, the models are reformulated using Bayesian methods. Gibbs sampling is used to integrate the prior over the likelihood to obtain the posterior distributions for the model parameters conditional on global temperature. Higher temperatures are conditionally associated with more strong hurricanes and higher return levels for the strongest hurricane winds. Results compare favorably with an ML approach as well as with recent modeling and observational studies. The maximum possible near-coastal wind speed is estimated to be 208 kt (183 kt) using the Bayesian (ML) approach.

1. Introduction

Coastal hurricanes are a serious social and economic concern for the United States. Strong winds, heavy rainfall, and storm surge kill people and destroy property. Hurricane destruction rivals that from earthquakes. In Florida alone Hurricane Andrew's strike in 1992 caused more than $30 billion in direct economic losses. Losses from the 2005 season are still being tallied. Historically, 80% of all U.S. hurricane damage is caused by 20% of the most intense hurricanes. The rarity of severe hurricanes implies that empirical estimates of return periods likely will be unreliable. Extreme value theory provides models for rare wind events and a justification for extrapolating to levels that are much greater than have already been observed. Definitive answers to questions about whether hurricanes will be more intense or more frequent in a future of global warming require long records. The longest records available are near the coast.

Probability estimates of extreme winds in tropical cyclones are available in the literature. Darling (1991) uses an empirical model to estimate local probabilities of hurricane wind speeds exceeding specified thresholds. Rupp and Lander (1996) use the method of moments on annual peak winds over Guam to determine the parameters of an extreme value model leading to estimates of recurrence intervals for extreme typhoon winds. Heckert et al. (1998) use the peaks-over-threshold method and a reverse Weibull distribution to

Corresponding author address: Dr. Thomas H. Jagger, Dept. of Geography, The Florida State University, Tallahassee, FL 32306. E-mail: tjagger@blarg.net

obtain mean recurrence intervals for extreme wind speeds at consecutive mileposts along the U.S. coastline. Chu and Wang (1998) use various parametric distributions to model return periods for tropical cyclone wind speeds in the vicinity of Hawaii. Jagger et al. (2001) use maximum likelihood (ML) estimation to determine a linear regression for the scale and shape parameters of the Weibull distribution for hurricane wind speeds in coastal counties. A Bayesian approach to estimate Weibull parameters from wind speed data is given in Pang et al. (2001).

The present study builds on these earlier works but differs in some crucial ways. First, we interpolate 6-hourly hurricane positions and intensities to 1 h. This allows us to determine the most extreme wind for hurricanes entering each region without adding a bias due to fixed regional boundaries. Second, we examine the effect of climate variables on the distribution of extreme winds. The model employed by Jagger et al. (2001) captures the variation of hurricane frequency as a function of climate variables using the Weibull distribution, which is appropriate for wind speeds above some threshold, but not necessarily appropriate for the most extreme winds. Here we attempt to put extreme hurricane winds in the context of climate variability and climate change. Third, we demonstrate the feasibility of a Bayesian approach for adding older, less reliable, data into the analysis.

This research attempts to answer the following questions: What are the return levels of maximum hurricane winds in near-coastal regions over 5, 10, 50, and 100 yr? Are the return levels different from region to region? What is the maximum possible hurricane wind speed level? How do these levels change under different climate conditions? In particular, although fewer hurricanes affect the United States when El Niño conditions are present, are they stronger? We answer these questions by statistically modeling the maximum wind speeds near the coast. We use an ML approach and use data only over the reliable period over records from 1899 to 2004. We then demonstrate the use of a Bayesian approach that allows us to incorporate an additional set of Atlantic hurricane data extending back to 1851. Results compare favorably with an ML approach and with recent modeling and observational studies.

The paper begins with a description of the data in section 2. Data used to characterize the dominant climate modes are also described. In section 3 we discuss the general assumptions behind our choice of models. In section 4 we describe the models including the generalized Pareto and generalized extreme value distributions. The choice of thresholds and measurement errors are discussed. Model results are shown in section 5. In section 6 we demonstrate how the analysis can be improved with the use of a hierarchical Bayesian specification. Summary and conclusions are presented in section 7. Although basic theory establishes an upper bound on the maximum hurricane intensity, here we estimate for the first time what that quantitative limit is.

2. Data

a. Maximum tropical cyclone intensity

Extreme value theory relies on asymptotic arguments for the behavior of the maximum observed value in a dataset (Palutikof et al. 1999). Here maximum wind speed estimates near the coast are derived from the Hurricane Database (HURDAT; or best track) maintained by the National Hurricane Center (NHC). HURDAT is the official record of tropical storms and hurricanes for the Atlantic Ocean, Gulf of Mexico, and Caribbean Sea, including those that have made landfall in the United States. HURDAT consists of the 6-hourly position and intensity estimates of tropical cyclones back to 1851 (Jarvinen et al. 1984; Neumann et al. 1999). For storms and hurricanes prior to 1931, the 6-h positions and intensities are interpolated from once-daily (1200 UTC) estimates. For storms in the period 1931–1956, the 6-h positions and intensities are interpolated from twice-daily (0000 and 1200 UTC) observations. Important revisions to the dataset (reanalysis), correcting systematic and random errors, are complete for the second half of the nineteenth century and early twentieth century (Landsea et al. 2004). Here we use the latest version of HURDAT as of December 2004, which includes reanalysis of all storms prior to 1911. For the initial models we use data over the reliable period, 1899–2004. When the models are reformulated using Bayesian methods, we include data over the less reliable 1851–98 period.

Despite the biases, these data have recently been used for hurricane risk analysis (Emanuel et al. 2006). In fact, we argue that we are on firmer ground here because we consider near-coastal hurricanes only, and we quantitatively consider the older data as less precise. Yet we would like to stress that the focus of our work is in providing the climate community with a modeling approach for quantifying return levels of the most extreme events. Whether or not we succeed should be judged independently of the perceived data quality.

As of this writing, the reanalysis of the HURDAT dataset does not contain a complete list of hurricane events by landfall location, time, and intensity so we develop an objective technique for estimating near-coastal wind speeds. First we divide the coast into three regions including the Gulf Coast, Florida, and the East

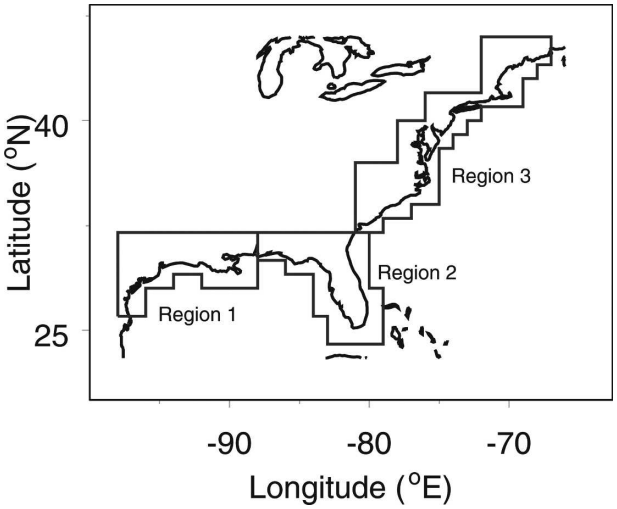

FIG. 1. Regions used in the study. The regions are chosen large enough to capture enough hurricanes, but small enough to show possible differences in extreme values between locations (e.g., Gulf vs East Coasts). The regional boundaries corresponding to whole number parallels and meridians. Region 1 is referred to as the Gulf Coast, region 2 as Florida, and region 3 as the East Coast.

Coast (Fig. 1). For notational purposes, we let the combined coastal regions of 1, 2, and 3 be denoted as region 4. Second, a natural spline interpolation is used to obtain positions and wind speeds at 1-h intervals from the 6-h values for all tropical cyclones in HURDAT. Third, for each of the hurricanes in the dataset, we note the maximum wind in each of four regions affected by a given hurricane. Fourth, for hurricanes with additional landfall intensities that exceed those from the 1-h interpolations, we manually add them to the dataset (e.g., Hugo in 1989 and Charley in 2004).

Considering only tropical cyclones with at least tropical storm force winds [>34 kt (17.5 m s^{-1}), where 1 kt = 0.514 m s^{-1}] over the period 1899–2004, this dataset contains $N = 875$ entries, for 383 tropical cyclones. Each entry $i = 1, \ldots, N$ is a quadruplet consisting of the region, r_i with values 1, . . . , 4, a sequential tropical cyclone identifier s_i, the year y_i, and the maximum wind w_i. By considering each region, $K = 1, \ldots, 4$ separately and ignoring the identifier, we generate four subsets of the data consisting of the pairs y_i, w_i, for $r_i = K$, denoted as $D(K)$. Associated with each entry is a row vector of yearly global climate factors $\mathbf{x}_{y_i}$ discussed below. Here the y_i subscript denotes that the values are the same for a given year, with $\mathbf{X}$ denoting the 106 (yr) $\times$ 4 factor matrix.

Figure 2 shows the histograms of annual maximum hurricane wind speeds for each region over the period 1899–2004. Counts are tallied in 10-kt intervals beginning with 65 kt. The counts do not sum to 106, as there are years without hurricanes near the coast. As expected there are more years when the maximum hurricane wind is less than 115 kt than greater than this value. In fact, during only 4 of the 106 yr did an East Coast hurricane produce winds in excess of 115 kt. This compares with 15 and 14 yr for the Gulf Coast and Florida, respectively. The distributions show a right (positive) skewness that is typical of rare events, but the decrease in counts as maximum wind speeds increase is different for each of the regions. Moreover the histograms are noisy (note the lack of wind maxima in the 95–105-kt range), making it problematic to get a reliable estimate of the return period of extreme winds directly from these distributions. The maximum wind speed in the dataset occurs at 171 kt (1-h spline interpolated value) for Hurricane Camille as it approached the northern Gulf Coast in 1969.

b. Climate factors

We argue that the return period of extreme near-coastal winds from a hurricane depends on climate factors. This is reasonable given that statistical relationships between U.S. hurricane counts and climate are well established (Elsner et al. 2004; Elsner 2003; Elsner et al. 2001, 2000a,b, 1999; Elsner and Kara 1999; Bove et al. 1998). More importantly for the present work, Jagger et al. (2001) model the typical wind speeds of hurricanes at landfall and show that over certain coastal counties the exceedance probabilities (e.g., wind speeds in excess of 100 kt) vary appreciably with ENSO and the North Atlantic Oscillation (NAO). Similarly, Murnane et al. (2000) model the probability of coastal hurricanes conditioned on ENSO. A study by Goldenberg et al. (2001) shows that the number and strength of Atlantic hurricanes follow a multidecadal cycle of changes in North Atlantic Ocean currents. This cycle, called the Atlantic Multidecadal Oscillation (AMO), is controlled by gradual changes in ocean currents. Of considerable interest to the scientific community and others is the influence, if any, global warming may have on the strongest hurricane winds (Pielke et al. 2005; Emanuel 2005; Webster et al. 2005). Thus, we include global temperature as a fourth climate factor.

For the present study, ENSO is characterized by basin-scale fluctuations in sea level pressure (SLP) between Tahiti and Darwin. Although noisier than equatorial Pacific sea surface temperature (SST), pressure values are available back to the middle of the nineteenth century. The Southern Oscillation index (SOI) is defined as the normalized sea level pressure difference between Tahiti and Darwin. The SOI is strongly anticorrelated with equatorial Pacific SSTs so that an El Niño warming event is associated with negative SOI

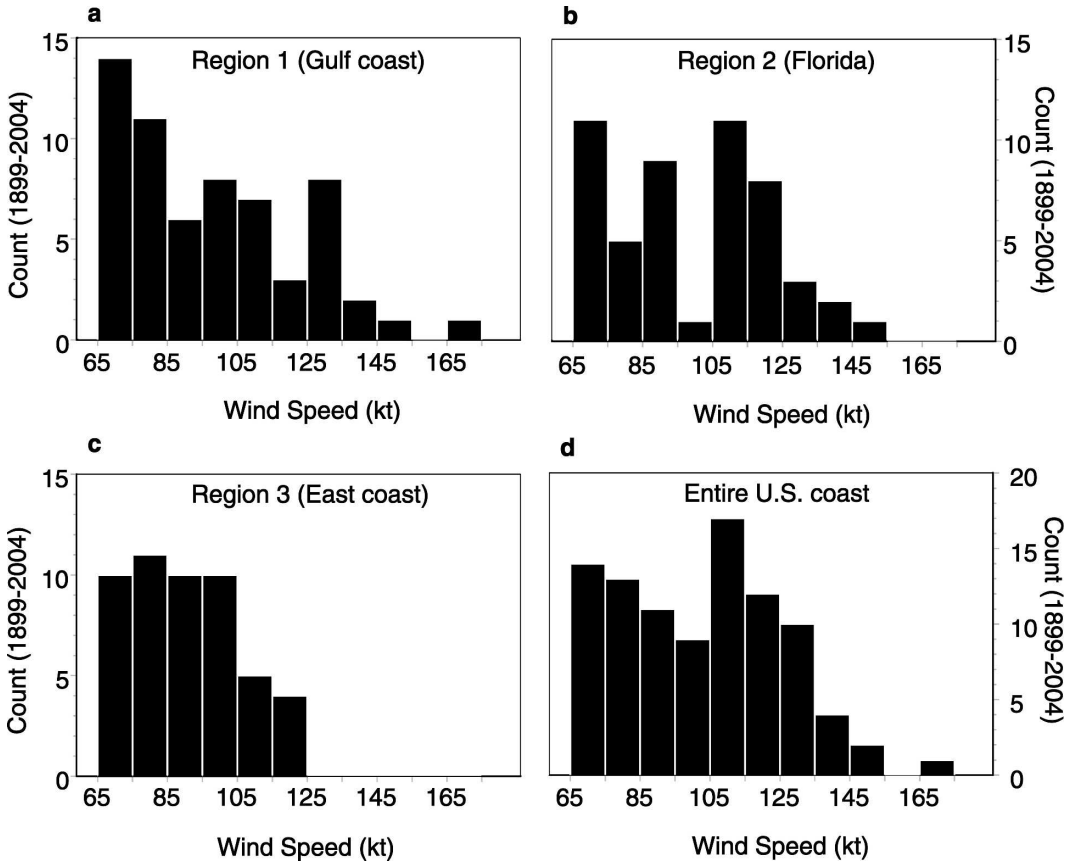

FIG. 2. Histograms of the annual maximum wind speed from hurricanes by region. The data include all hurricanes in the best-track (HURDAT) dataset over the period 1899–2004. If two or more hurricanes are tracked through the region, only the highest wind speed is used for these plots.

values. Units are standard deviations. The relationship between ENSO and hurricane activity is strongest during the hurricane season, so we use an August–October average of the SOI as our predictor. The monthly SOI values (Ropelewski and Jones 1987) are obtained from the Climatic Research Unit (CRU).

The NAO is characterized by fluctuations in sea level pressure differences. Index values for the NAO are calculated as the difference in SLP between Gibraltar and a station over southwest Iceland, and are obtained from the CRU (Jones et al. 1997). The values are averaged over the pre- and early hurricane season months of May and June (Elsner et al. 2001). Physically we speculate that the relationship might result from a teleconnection between the midlatitudes and Tropics whereby a below-normal NAO during the spring leads dry conditions over the continents and to a tendency for greater summer/fall middle-tropospheric ridging (enhancing the dry conditions). Ridging over the eastern and western sides of the North Atlantic basin during the hurricanes season tends to keep the middle-tropospheric trough, responsible for hurricane recurvature, farther to the north (Elsner and Jagger 2006a,b).

The AMO is characterized by fluctuations in SST over the North Atlantic Ocean driven largely by the thermohaline circulation. The Hadley Centre model SST and National Oceanic and Atmospheric Administration (NOAA) optimal interpolated SST datasets are used to compute Atlantic SST anomalies in degrees Celsius north of the equator (Enfield et al. 2001). Anomalies are computed by month using the base period 1951–2000. Data are obtained online from the NOAA–Cooperative Institute for Research in Environmental Studies (CIRES) Climate Diagnostics Center back to 1871. For this study we average the SST anomalies over the peak hurricane season months of August through October. Monthly global temperature anomalies (1961–90 base period) from the Intergovernmental Panel on Climate Change (IPCC) values are obtained from the CRU back to 1856 (Folland et al. 2001). Here we average the global temperature anomalies in degrees Celsius over the months of August–October. The

anomalies are accurate to ±0.05°C for the period since 1951, but are about 4 times as uncertain during the 1850s.

In summary, the distribution of extreme near-coastal hurricane winds will be modeled using extreme value theory using data initially from the period 1899–2004. Additionally, the August through October averaged values of the SOI, the AMO, and global temperature along with the May through June averaged values of the NAO will be used to examine differences in the extreme distributions depending on whether these climate variables are above or below normal during this 106-yr period. Therefore the climate variables enter the model as binary factors (above or below normal) rather than continuous covariates. Using binary factors makes it easier to interpret the results. It also provides an initial examination of the relationship between climate variables and extreme value distributions without having to specify the relationship of the model coefficients to the indices.

For reference, the upper and lower quartile values of the SOI are 0.41 and −0.89 standard deviations (std dev), respectively, with a median (mean) value of −0.19 (−0.16) std dev. Years of below- (above) normal SOI correspond to El Niño (La Niña) events and thus to lower (higher) probability of near-coastal hurricanes. The upper and lower quartile values of the NAO are 0.42 and −1.08 std dev, respectively, with a median (mean) value of −0.39 (−0.32) std dev. Years of below- (above) normal values of the NAO correspond to a weak (strong) NAO phase and thus to higher (lower) probability of near-coastal hurricanes. The upper and lower quartile values of the AMO are 0.13° and −0.21°C, respectively, with a median (mean) value of −0.02°C (−0.03°C). Years of above- (below) normal values of the AMO correspond to higher (lower) probability of basinwide hurricane activity. The upper and lower quartile values of the global temperature are 0.06° and −0.22°C, respectively, with a median (mean) value of −0.06°C (−0.05°C). The correlations of the indices used in the model are shown in Table 1. The linear correlation between the SOI and the NAO (AMO) is a negligible −0.02 (−0.01). The linear correlation between the NAO and the AMO is −0.14. The correlation between the SOI and global temperature (GT) is −0.13. The only significant correlation is between the AMO and GT with a value of +0.79.

TABLE 1. Correlations between climate indices. Values are the linear correlation coefficient using data from 1899–2004. The p value is based on the null hypothesis of zero correlation.

Indices	Correlation	p value
SOI, NAO	−0.02	0.826
SOI, AMO	−0.01	0.942
SOI, GT	−0.13	0.190
NAO, AMO	−0.14	0.144
NAO, GT	−0.07	0.457
AMO, GT	+0.79	0.000

3. Hurricane data assumptions

A brief discussion of a point process is important for understanding the statistical model and its limitations. We model the hurricane dataset as a marked Poisson process in which the events are hurricanes and where each mark is the maximum wind speed of a hurricane within a region. We make some assumptions of the independence of the marks and the underlying process as well as between the marks themselves (Cressie 1993).

Each dataset $D(K)$ can be considered as a sample from a spatial point process, $\mathcal{D}$, over the two-dimensional space composed of the integers and positive reals, that is, $\mathbb{N} \times \mathbb{R}^+$, restricted to the rectangular region, $[1899, 2004] \times \mathbb{R}^+$. Using the idea of a spatial point process we can define useful quantities. For instance, the activity for year y of all tropical cyclones with maximum winds exceeding u is the number of points, $N(y, u)$ from a realization of $\mathcal{D}$ inside the region $(y \times [u, \infty])$. Thus, $N(y, u)$ represents a family of random variables on the positive integers, and $N(y, 64)$ is the annual number of hurricanes for year y. We can view the problem of finding the maximum yearly wind speed by fixing the threshold, u, and noting that the distribution of the yearly maxima can be determined from the distribution of $N(y, u)$ and the distribution of the maximum winds given that the maximum winds exceed u. If u is large enough, then for all practical purposes, $N(y, u)$ takes on only values of zero and one, so based on a conditioning argument, the probability that the maximum wind W exceeds a value v is $\Pr[N(y, u) = 1] \times \Pr(W > v | W > u)$. This is called the peaks-over-threshold method (McNeil and Saladin 2000).

Additional assumptions are necessary. First, we assume that the occurrence of a hurricane within a coastal region is independent of future hurricane occurrences in the same region. Second, we assume that hurricane intensity is independent so that the intensity of a previous hurricane has no bearing on the intensity of a future hurricane. Thus, while the interpolated hurricane intensities along a particular hurricane track are not independent, the maxima from one hurricane to the next are. Then, the two-dimensional spatial process describing set $D(K)$ can be described as a two-dimensional Poisson process over $\mathbb{N} \times \mathbb{R}^+$ with an associated mean measure $\Lambda_K(A)$. For example, if $A = [1901, 2000] \times [64, \infty]$, then $\Lambda_K(A)$ is the expected number of hur-

ricanes in the twentieth century occurring within region K. Since $D(K)$ is a Poisson process, the number of hurricanes observed during this century for region K has a Poisson distribution with a mean value of $\Lambda_K(A)$. Another feature of the Poisson process is that the probability of a single event B occurring in a smaller region contained in A is just $\lambda_K(B)/\lambda_K(A)$; thus if a single hurricane occurs in year y, then $\Pr(W > v|W > u) = \Lambda_K(y, [v, \infty])/\Lambda_K(y, [u, \infty])$. We also assume that the maximum wind speed has a continuous distribution so our process has an associated intensity λ_K where $\Lambda_K([a, b] \times [c, d]) = \Sigma_a^b \int_c^d \lambda_K(y, w)dw$. So our count $N(y, u)$ is a Poisson random variable with mean $\int_u^\infty \lambda_K(y, w)dw$. Finally, we assume that in a given year, tropical cyclone occurrence is a function of the set of yearly climate variables and the wind speed w, so that the intensity in each coastal region, λ_K, can be expressed as $\lambda_K(y, w) = \lambda_K(\mathbf{x}_y, w)$.

The above assumptions imply that if we have knowledge of the climate factors and of the spatial process of hurricane intensity we have sufficient information for answering the questions we stated in the introduction. For example, what is the 100-yr return period for hurricane winds in a given region, assuming that a climate factor such as the AMO is above normal during these 100 yr? We can determine the return level by solving $\Lambda_K([1, 100] \times [u, \infty]) = 1$ for u. If we assume that a particular climate factor is the same for each of these 100 yr (e.g., above normal), then the problem is to solve $0.01 = \int_u^\infty \lambda_K(\mathbf{x}, w)dw$. This form is natural for finding the distribution of maximum values. We let $\Pr(M_Y \leq u)$ denote the probability that the maximum winds observed over Y years (M_Y) under a given climate scenario ($\mathbf{x}$) are less than or equal to u; that is, no hurricanes occur in Y years with winds exceeding u. Since the distribution of events with wind exceeding u is Poisson with mean $r = Y\int_u^\infty \lambda_K(\mathbf{x}, w)dw$, then $\Pr(M_Y \leq u) = \exp(-r)$. Also, by the nature of a Poisson process, if a single hurricane occurs with winds exceeding u, then the probability that the winds exceed v are $\int_v^\infty \lambda_K(\mathbf{x}, w)dw/\int_u^\infty \lambda_K(\mathbf{x}, w)dw$. When $u = 0$ the denominator is the yearly hurricane rate and $\lambda_K(\mathbf{x}, w)/\int_0^\infty \lambda_K(\mathbf{x}, v)dv$ is the probability density of the maximum wind at w.

4. Extreme value theory

a. Introduction

Extreme value theory is a discipline within statistics. It is unique in that it concerns techniques and models for describing the rare event rather than the typical (average) event. During the 1950s it was used by civil engineers to provide a framework for estimating the likely forces on built structures using historical data. Extreme value theory and the central limit theory are derived in a similar manner. Both consider the limiting distributions of independent identically distributed (iid) random variables under an affine transformation.[1] According to the central limit theorem, the mean value of a sample of iid random variables x_i converges to a normal distribution with mean 0 and variance 1 under the affine transformation $(\bar{x} - \mu)/\sqrt{n\sigma^2}$, where μ and σ are the mean and standard deviation of x_1, respectively. Correspondingly, if the distribution of the maxima under some affine transformation converges, then it must converge to a member of the generalized extreme value (GEV) family of distributions (Embrechts et al. 1997). The maxima of most continuous random variables converge to a nondegenerate random variable. Incidentally, this is not the case for the maxima of commonly used discrete random variables including the Poisson, geometric, and negative binomial.

In the absence of empirical or physical evidence for assigning an extreme level to a process, an asymptotic argument is used to generate extreme value models. But extreme values are scarce, making it necessary to estimate levels that are much higher than what already have been observed. In fact, the goal of an extreme value analysis is to quantify the statistical behavior of processes at unusually high levels. In particular, extreme value analysis requires an estimation of the probability of events that are more extreme than any that have ever been observed. This implies an extrapolation from observed levels to unobserved levels. Extreme value theory provides a family of models to make such extrapolation. In fact there are no more serious competitor models than those provided by extreme value theory (Coles 2001). Hurricane climatologists, instead, tend to rely on a set of summary statistics when analyzing extreme events (Chan and Liu 2004; Landsea et al. 1999).

Given a set of observations from an unknown but continuous random process, if we generate a sample from the set, take the maximum value from the sample, and repeat the procedure many times, we obtain a distribution that is different from that of the original (parent) distribution. The distribution of the maximum will be shifted to the right and the shape (skewness) will change. For instance, if the original distribution is normal, the limiting shape becomes Gumbel. The new location, shape, and scale of the maximal distribution are determined by the tail behavior of the parent distribution [see Rupp and Lander (1996) for an example]. In fact, we can simplify the description of the tail behavior

[1] Linear transformation followed by a translation.

by using three parameters for the family of GEV distributions. Thus there is a need to consider maximal distributions if one is interested in describing extreme values of the parent distribution. Fortunately, there is a family of distributions that is the limiting distribution of these maxima.

Of interest is the stationary set of distributions arising from the family of GEV functions that represent the limiting behavior of the maxima of a collection of iid random variables. The GEV distributions have continuous densities so they can be used in Bayesian analysis with continuous or discrete priors since the product of the likelihood and prior is integrable. More generally, methods exist in which samples of the posterior distributions of the GEV parameters can be generated (Coles 2001).

b. Generalized Pareto distribution

Whereas the GEV family of distributions expresses the limiting behavior of the maximum value of a set of observations, the family of generalized Pareto distributions (GPDs) describes the behavior of individual extreme events. Consider observations from a collection of iid random variables in which we keep only those observations that exceed a fixed threshold value (not just the maximum as we did in the discussion above). As we increase the threshold, the two-parameter GPD family represents the limiting behavior of this new collection of random variables. This makes the family of GPDs a suitable choice for modeling extreme events. The GPD and GEV distributions are related. A GEV distribution results from a GPD when we consider the maximum over a fixed period of time from a marked Poisson process in which the marks are iid samples from a GPD. Conversely, consider an increasing collection of iid random variables location shifted and scaled so that the maximum converges to a member of the family of GEV distributions. The subset of this collection of random variables, after subtracting the threshold value and discarding all resulting values less than zero, converges to a member of the GPD family (Coles 2001).

In discussing the GPD we have introduced the idea of a threshold. Observations below the threshold value are removed from the analysis. The choice of threshold is a compromise between retaining enough observations to properly estimate the distributional parameters, but few enough that the observations follow a GPD family. More specifically, we are modeling the exceedances, $W - u$, as samples from a family of GPDs so that for an individual hurricane with maximum winds W,

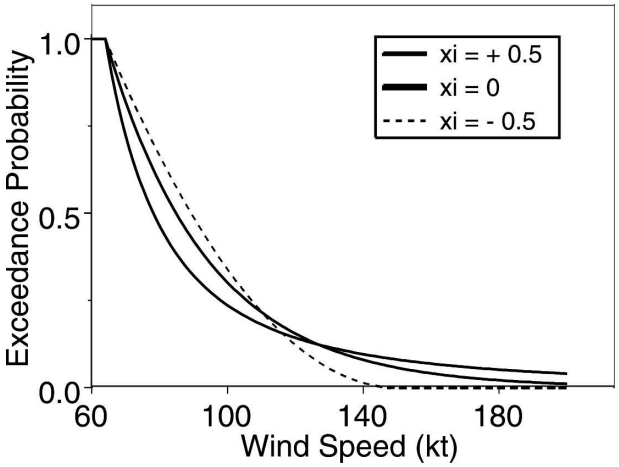

FIG. 3. Examples of GPD exceedance curves. The bold curve is for $\xi = 0$ and is exponential. The thin line is $\xi = +0.5$ and the dashed line is $\xi = -0.5$. Of interest is the fact that the tail behavior is different for different values of ξ. The threshold is 64 kt.

$$\Pr(W > v | W > u) = \begin{cases} \exp[-(v-u)/\sigma] & \text{when} \quad \xi = 0 \\ \left[1 + \dfrac{\xi}{\sigma_u}(v-u)\right]^{-1/\xi} & \text{otherwise} \end{cases} \tag{1}$$

$$= \mathrm{GPD}(v - u | \sigma_u, \xi), \tag{2}$$

where $\sigma_u > 0$ and $\sigma_u + \xi(v - u) \geq 0$. Since this model is true for any u we have

$$\sigma_u = \sigma_0 + \xi \times u$$
$$\xi_u = \xi.$$

The parameters σ_u and ξ are referred to as the scale and shape parameters, respectively. For negative shape parameters the GPD family of distributions has an upper limit of $W_{\max} = u + \sigma_u/|\xi|$.

To illustrate these distributions, Fig. 3 shows plots of exceedance distributions for three values of ξ. The abscissa is wind speed and the ordinate is exceedance probability. For $\xi = +0.5$ the tail is fat, meaning the exceedance probability drops off fast for weaker wind speeds, but more slowly for higher wind speeds. For $\xi = 0$, the drop-off is exponential. For $\xi = -0.5$ the curve is bounded on the right, meaning that the exceedance probability is zero beyond a certain wind speed.

c. Full model

The above GPD describes the maximum wind distribution for each hurricane whose winds exceed u but not the frequency of hurricanes at that intensity. From our assumptions, the number of hurricanes in year y whose maximum winds in region K exceed u have a Poisson distribution with mean (or exceedance) rate $\lambda_u = \Lambda_K(y, [v, \infty])$. Thus by combining the exceedance probability

and the exceedance rate with our assumption that the exceedances are independent we get the number of hurricanes per year with winds exceeding v, and N_v has a Poisson distribution with mean

$$\lambda_v = \lambda_u \times \Pr(W > v | W > u). \quad (3)$$

This specification is physically realistic since it allows us to model hurricane occurrence separately from hurricane intensification. Moreover from a practical perspective, rather than a return rate per hurricane occurrence, the above specification allows us to obtain an annual return rate on the extreme winds, which is more meaningful for the business of insurance.

Now, the probability that the yearly maximum will be less than v is the probability that $N_v = 0$. Since N_v has a Poisson distribution

$$\Pr(W_{\max} \le v) = \Pr(N_v = 0) \quad (4)$$

$$= \exp(-\lambda_v) \quad (5)$$

$$= \exp[-\lambda_u \times \mathrm{GPD}(v - u | \sigma_u, \xi)]. \quad (6)$$

If we make the substitutions for $\xi \neq 0$,

$$\sigma_\mu = \lambda_u^\xi \times \sigma_u$$

$$\mu = u + \frac{\sigma_\mu - \sigma_u}{\xi},$$

then

$$\Pr(W_{\max} \le v) = \exp\left\{-\left[1 + \xi\left(\frac{v - \mu}{\sigma_\mu}\right)\right]^{-1/\xi}\right\} \quad (7)$$

has a GEV distribution, which is in canonical form. If $\xi = 0$, then we make the substitutions

$$\sigma_\mu = \sigma_u$$

$$\mu = u + \sigma_u \times \log(\lambda_u)$$

then

$$\Pr(W_{\max} \le v) = \exp\left\{-\exp\left[-\left(\frac{v - \mu}{\sigma_\mu}\right)\right]\right\}. \quad (8)$$

We convert the peaks-over-threshold parameters λ_u, σ_u, and ξ to the GEV canonical parameters μ, σ_μ, and ξ, and so compare results obtained with different thresholds. Using the canonical parameters, for example, we calculate the yearly (seasonal) return level, $\mathrm{rl}(r)$, corresponding to a given return period, r and GEV parameters μ, σ, and ξ by solving for v in $\Pr(W_{\max} \ge v) = 1/r$, giving

$$\mathrm{rl}(r) = \begin{cases} \mu + \dfrac{\sigma}{\xi}\left\{\left[\log\left(\dfrac{r}{r-1}\right)^{-\xi} - 1\right]\right\} & \xi \neq 0 \\ \mu - \sigma \times \log\left[\log\left(\dfrac{r}{r-1}\right)\right] & \xi = 0. \end{cases} \quad (9)$$

Additional details are given in Coles (2001).

5. Return levels for extreme hurricane winds

a. Threshold determination

The extreme value models described in the previous section have a fixed threshold value u that needs to be determined. Here the mean residual life (MRL) plot is used to determine the threshold. The MRL plot is produced by averaging the difference in the observed wind speeds above a specified level (residual) as a function of the level. For example, at a wind speed level of 50 kt we subtract 50 from each observed wind speed and average only the positive values (excesses). We repeat for all wind speed levels. The mean excess is the expected value of the amount that the observations exceed the particular level. The standard errors on the mean excess allow us to compute confidence levels for the estimates. A nearly straight-line negative relationship between the mean residual and the wind speed level above some threshold indicates the set of extreme wind speeds. In other words, if extreme values follow a GPD, then their expected value is a linear function of the threshold; that is,

$$E(Y - u) = \frac{\sigma_0 + \xi u}{1 - \xi}$$

$$= \frac{\sigma_0}{1 - \xi} + \frac{\xi}{1 - \xi} \times u$$

according to Coles (2001). The MRL plot can be used to get estimates for the GPD parameters, σ and ξ.[2]

Figure 4 shows the relationship between the mean excess and the threshold for the three regions and for the entire coast using the list of observed maximum wind speeds over the period 1889–2004. The jaggedness of the curves result from the 5-kt precision on the wind speed estimates in HURDAT. The thin lines represent 95% confidence limits. For the Gulf Coast and Florida regions a straight-line fit to the curve starts at a level between approximately 75 and 90 kt. For the East Coast region the straight-line fit starts near 65 kt and for the entire coast the straight line fit starts between 90 and 100 kt. Thus we choose the nearest Saffir–Simpson category for the threshold: 83 kt (category 2) for the Gulf Coast and Florida, 64 kt (category 1) for the East Coast, and 96 kt (category 3) for the entire coast. An alternate method is to calculate the parameters of the GPD distribution using either the ML estimator or the method of probability-weighted moments for a sequence of threshold values. The first location at which

[2] Here, σ_u for any value of u can be found using $\sigma_u = \sigma_0 + \sigma(0) + u \times \xi$, whereas ξ remains constant.

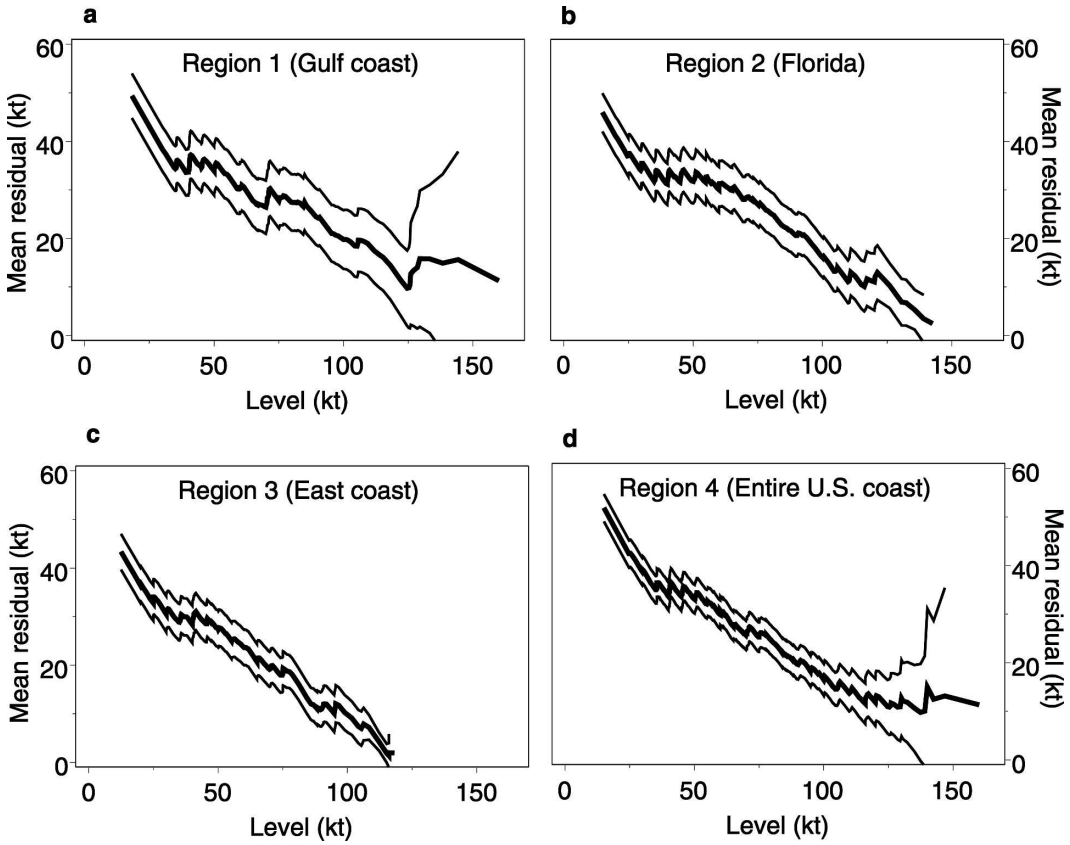

FIG. 4. Mean residual life plots for near-coastal hurricane winds by region. The thin lines are the 95% confidence limits. An approximate linear decrease of the mean excess occurs for a threshold of (a), (b) 83 kt (category 2) for regions 1 and 2, (c) 64 kt (category 1) for region 3, and (d) 96 kt (category 3) for region 4 (entire coast).

the parameter values stabilize is a reasonable threshold value (Coles 2001; Greenwood et al. 1979). Results from this method are consistent with those from the MRL plots.

We use the maximum likelihood method based on Coles (2001) to estimate the model parameters but augment it to handle threshold-crossing (exceedance) rate as needed for the return levels. The 95% confidence bands for the return levels are calculated using a delta method from the covariance matrix of the parameters generated by this software. Unfortunately, the covariance matrix, being the scaled inverse of the Hessian matrix, is not always available using this method because the Hessian matrix is nonsingular. In such cases we cannot compute confidence bands for the parameters or for the return levels. Thus our ML approach is limited to using binary factors.

b. Models for climatology

Figure 5 shows return level plots of extreme hurricane winds by region. The return level (ordinate) has units of wind speed in knots and the return period (abscissa) is given in years. The return level is expected to be exceeded on average once every return period. Expressed another way, the annual probability of winds exceeding the 10-yr return level is 0.1. The middle curve is the mean return level for a given return period, and the outside thin lines are the 95% confidence limits. The curves asymptote to finite levels as a consequence of a negative estimate for the value of ξ, though each region displays a somewhat different curve shape. The panels have identical scales for easier visual comparisons. Points on the graphs are the observed maximum wind speeds and are placed along the abscissa using empirical return period estimates. Empirical return period estimates are made using the reciprocal of the return rate, which is the product of the yearly hurricane rate times the exceedance probability. The yearly rate is the number of hurricanes divided by the record length in years. The exceedance probability for a particular hurricane wind speed is approximated by dividing the rank of the hurricane wind speed (the maximum wind speed has a rank of 1) in the record by the number of hurricanes after subtracting 0.5 from the rank. Thus

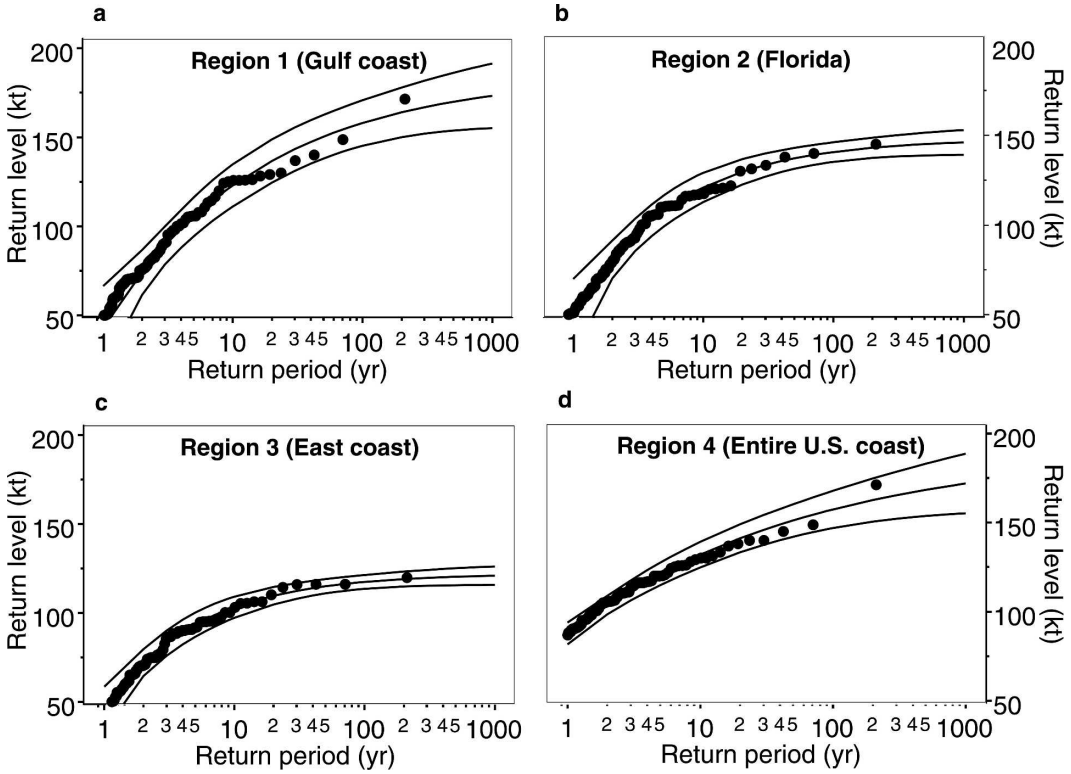

FIG. 5. (a)–(d) Return level plots by region. The curves are based on an extreme value model and asymptote to finite levels as a consequence of a negative estimate for ξ. Parameter estimates are made using the ML approach. The thin lines are the 95% confidence limits. The return level is the expected maximum hurricane intensity (kt) over p years. The points are the empirical estimates.

with N years, the approximate return period for a wind speed x is $\{N/[\text{rank}(x) - 0.5]\} + 0.5$. In general the points fall close to the curves, indicating that the models fit the data well.

Return levels for return periods greater than 10 yr are highest for the Gulf Coast region and smallest for the East Coast. Florida's return level curve is similar to the return level curve from the Gulf Coast, but Florida return levels are somewhat higher for short return periods and lower for the longest return periods. The mean return levels for various return periods are tabulated in Table 2. The 5-yr return levels are 105 kt for the Gulf Coast, 108 kt for Florida, and 93 kt for the East Coast. On average the entire U.S. coast is threatened by a 121-kt hurricane once every 5 yr. The 50-yr return levels are 150 kt for the Gulf Coast, 137 kt for Florida, and 115 kt for the East Coast. The 500-yr return levels increase to 170 kt for the Gulf Coast, 145 kt for Florida, and 120 kt for the East Coast. The Gulf Coast model gives a mean 1000-yr return level of 173 kt with a 95% confidence limit of 191 kt. It should be kept in mind that these extreme wind extrapolations are based on hurricanes near the coast and may represent a slightly high bias with respect to landfall winds. On the other hand, since the HURDAT observations (or interpolations) are only every 6 h, it is possible that there is low bias for rapidly intensifying hurricanes near the coast. Regardless, the uncertainty on the return levels indicated by the 95% limits should be regarded as a lower bound since the uncertainty could by much greater if the uncertainty due to model choice is also included (Coles 2001).

TABLE 2. Hurricane return levels by region. Values (kt) are based on a GPD model for the maximum wind distribution for each hurricane and a Poisson model for the yearly hurricane rate. Model parameters are estimated using the ML method. Values to the right of the ± refer to half the 95% confidence interval.

Return period (yr)	Region 1 Gulf Coast	Region 2 Florida	Region 3 East Coast	Region 4 Entire coast
5	105 ± 11	108 ± 9	93 ± 7	121 ± 6
10	123 ± 12	121 ± 8	103 ± 6	132 ± 7
50	150 ± 12	137 ± 6	115 ± 4	151 ± 9
100	158 ± 13	141 ± 5	117 ± 4	157 ± 10
500	170 ± 16	145 ± 6	120 ± 5	168 ± 15

TABLE 3. Same as in Table 2, except that the values refer to the conditional return levels (kt). Values are the result of independent conditioning on the SOI, NAO, AMO, and global temperature as discrete factors (above and below normal).

Return period (yr)	SOI		NAO	
	Above	Below	Above	Below
5	125 ± 5	116 ± 12	120 ± 9	123 ± 9
10	131 ± 5	130 ± 14	130 ± 9	134 ± 10
50	138 ± 4	156 ± 18	143 ± 6	154 ± 14
100	140 ± 4	164 ± 21	146 ± 8	161 ± 16
500	142 ± 6	178 ± 34	150 ± 10	173 ± 25
Return period (yr)	AMO		GT	
	Above	Below	Above	Below
5	125 ± 9	118 ± 9	120 ± 10	123 ± 8
10	136 ± 11	127 ± 9	132 ± 11	132 ± 8
50	156 ± 13	140 ± 8	154 ± 16	144 ± 7
100	162 ± 16	144 ± 9	161 ± 20	147 ± 7
500	173 ± 22	148 ± 14	175 ± 30	151 ± 11

c. *Models with climate factors*

Here we reproduce the return level plots but separate the observations into two factors based on whether the individual climate variable is above or below average during the hurricane season. We begin by considering the entire coast (Fig. 6) with mean return levels in Table 3. Results show that the most substantial differences in return levels occur with the SOI factor. For short return periods (less than 5 yr), above-normal SOI values (La Niña conditions) are associated with higher return levels (stronger hurricanes), but for longer return periods (greater than 30 yr), below-normal SOI values (El Niño) are associated with the higher return levels. These results align with our expectations that El Niño conditions are associated with less hurricane activity. Interestingly, however, El Niño conditions are associated with the most extreme hurricane winds. Although El Niño tends to inhibit hurricane formation (Gray 1984) through increased tropospheric wind shear (Goldenberg and Shapiro 1996), the accompanying lower-stratospheric cooling may increase the potential intensity of hurricanes that do form.

Differences in return levels are also noted with the NAO factor. Here below-normal values of the NAO are associated with higher return levels for all return periods, with the most significant differences occurring for the shortest and for the longest return periods. This is consistent with the results of Elsner and Jagger (2006a,b). As expected, years of above-normal values for the AMO are years with stronger hurricanes for all return periods. Compared with the return level differences noted for the SOI, the differences for the AMO are less between warm and cold years. Similarly global temperatures suggest higher wind speeds for the strongest hurricanes (maximum winds in excess of 135 kt) during above-normal years.

Care should be exercised in interpreting these results, especially for the AMO and global temperatures. As mentioned above, there is a significantly high correlation between the AMO and global temperature. That is, years of above- (below) normal AMO tend to coincide with years of above- (below) normal global temperature. Here we make no attempt to control for the AMO when examining the wind speed results conditional on global temperature. On the other hand, the results are consistent with theoretical arguments suggesting an increase in the maximum potential intensity of hurricanes with global warming through changes in surface and upper-tropospheric energy fluxes (Emanuel 1987; Lighthill et al. 1994; Henderson-Sellers et al. 1998). In fact a statistical analysis suggests that increases in the potential hurricane intensity will likely lead to an increase in actual hurricane intensity (Emanuel 2000) and a recent modeling study indicates the potential for a small increase in future hurricane wind speeds (Knutson and Tuleya 2004) as a consequence of global warming. Our results are also consistent with recent observational studies showing increases in the frequency and/or duration of the strongest hurricanes (Emanuel 2005; Webster et al. 2005).

Figure 7 shows the return level plots for regions 1, 2, and 3 and for the two climate factors SOI and NAO. To make the comparisons easier, we remove the 95% confidence lines. We see that for each of the regions, El Niño (below-average SOI) conditions are associated with lower return levels with the exception of extreme hurricanes along the Gulf Coast, which have a lower return period for a given extreme wind speed. In contrast, Florida hurricane activity appears to be most strongly influenced by the phase of the NAO. For a given wind speed, return periods are shorter (longer) when the NAO is below (above) average. Similar results are noted for the Gulf Coast, but not for the East Coast.

The above results are based on models from extreme value theory with inferences made using the ML estimates for the model parameters. We are motivated to consider another inferential method because 1) the standard error estimates from the ML method are biased (in fact, for some regions, the method fails to give values for the standard errors), 2) we would like to include the older, less precise data records from the nineteenth century in the analysis, and 3) we would like to treat the predictors as continuous covariates rather than as discrete factors. Next we reformulate the extreme value models using a Bayesian approach.

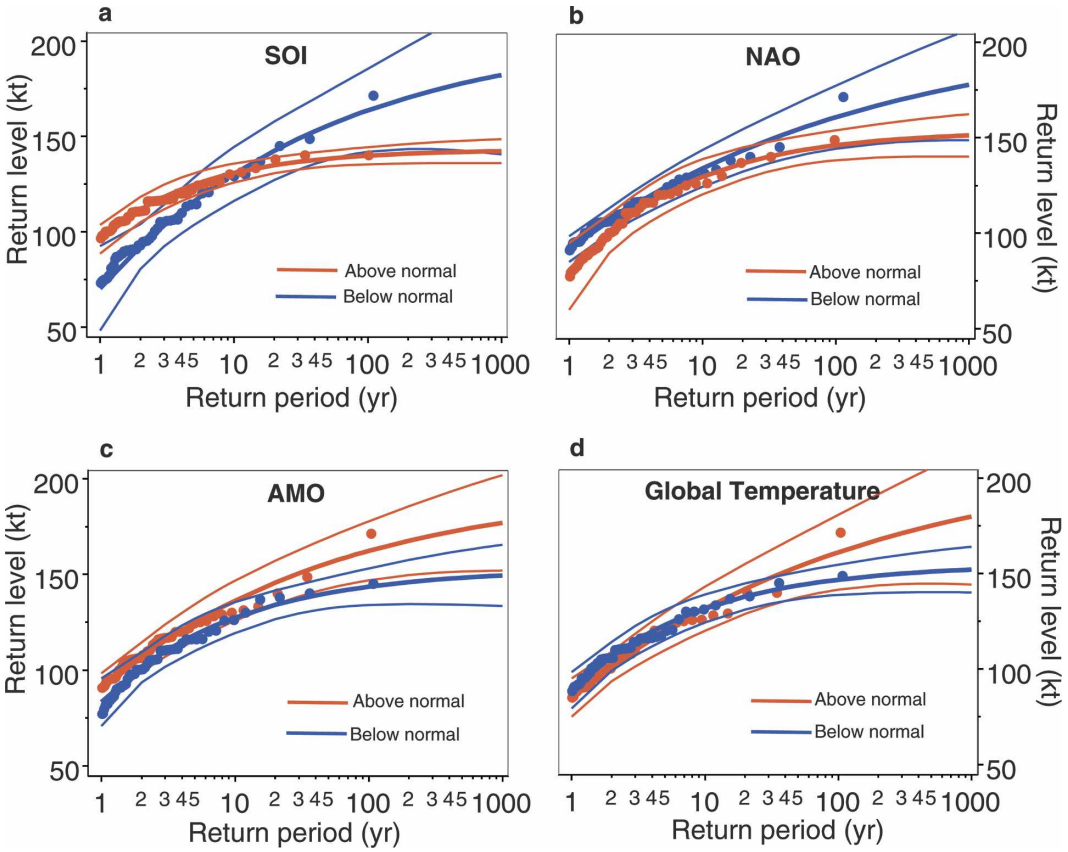

FIG. 6. (a)–(d) Return level plots for the entire U.S. coast (region 4) by climate factors. The curves are based on an extreme value model using an ML estimation procedure. Red (blue) lines and points indicate above- (below) normal climate conditions.

6. A Bayesian approach

a. Background and motivation

Applications of Bayesian extremal analysis are still relatively rare (Coles and Tawn 1996; Katz et al. 2002; Coles et al. 2003). In the context of local hurricane winds, Casson and Coles (1999) use a Bayesian analysis to estimate parameters of spatial regression models. They show that including the spatial characteristics of extremes provides a substantial reduction in the confidence intervals for high quantiles. A Bayesian approach to modeling extreme wind behavior is given in Walshaw (2000). They use a mixture model for extreme winds arising from pressure gradients and tropical cyclones at two separate locations (Key West, Florida, and Boston, Massachusetts). The approach allows them to incorporate prior information available from nearby sites. Here we restrict our data to winds from tropical cyclones eliminating the need to consider a mixture model. Since parameter estimates in extreme value theory are sensitive to large, rare events, the ability to include long historical records is particularly important in modeling extreme events. The utility of the Bayesian approach for modeling the mean number of coastal hurricanes is shown in Elsner and Jagger (2004).

The Bayesian approach to inference from extreme value models has several advantages over the ML approach used in the previous section. First, the facility to include other sources of less reliable data has obvious appeal. Second, the posterior distribution gives a more complete inference than the corresponding ML analysis (Coles 2001). In particular, for an estimate of future hurricane wind risk, expression of results using predictive distributions is advantageous. Third and more technical, Bayesian specifications do not depend on the regularity assumptions required by asymptotic theory of maximum likelihoods. The superiority of adopting a Bayesian inferential approach to extreme value analysis is shown in Coles and Pericchi (2003).

b. A hierarchical specification

To utilize a Bayesian approach for peaks-over-threshold extreme value modeling of near-coastal hurricane winds, we employ a hierarchy. At the bottom,

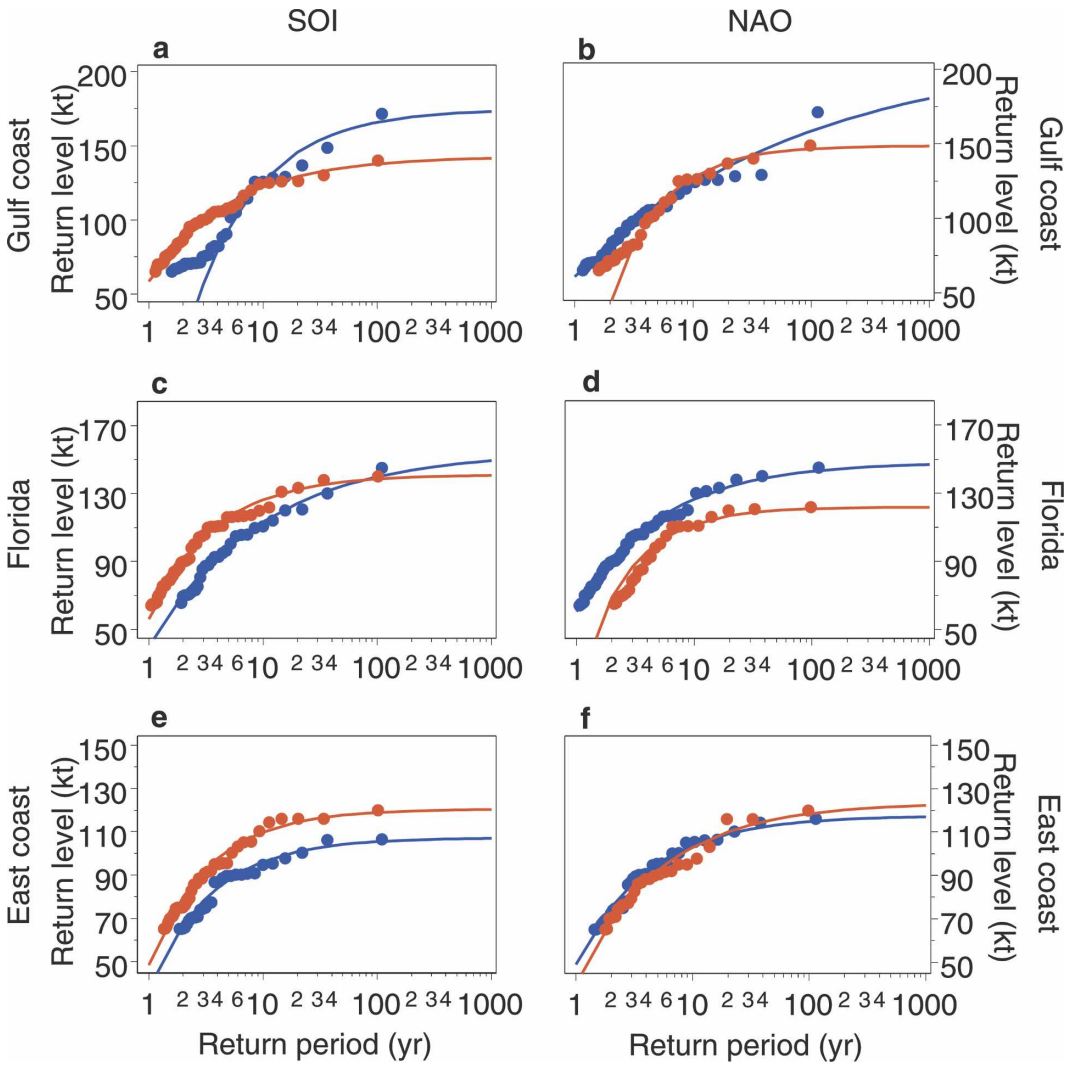

FIG. 7. Return level plots for (a), (b) region 1, (c), (d) region 2, and (e), (f) region 3 by climate factors. The curves are based on an extreme value model using an ML estimation procedure. Red (blue) lines and points indicate above- (below-) normal climate conditions. Panels (a), (c), and (e) [(b), (d), and (f)] are for the SOI (NAO) as a factor.

the maximum wind speed along a track in the coastal region, W_i, is uniformly distributed about the "true" but unobserved wind speed w_i. This uniform distribution is bounded by the observational error, e_i, so that W_i is uniformly distributed between $w_i \pm e_i$. Having no additional information about the observational error except for rounding, we use only the rounding error.

At the next level of the hierarchy we specify that w_i depends on the parameters of the GPD. For this initial modeling experiment we consider the entire coast only and restrict the analysis to global temperature as a single covariate. Thus, we fix the threshold wind speed (u) at 96 kt and employ a simple missing data model using a normal reference distribution for the global temperature. This allows us to use the full HURDAT record to 1851 despite the fact that global temperature values are available only as far back as 1856. Since the GPD has a closed form, the above hierarchical specification provides a method of generating predictive samples as well as samples of the exceedance probabilities and distributions for return levels.

To complete the hierarchy we model the exceedance rate (threshold crossing). Since we fix u and we assume that the priors on the two sets of parameters (hurricane frequency parameter is independent of hurricane intensity parameters) are independent, the posterior joint distributions on the parameters are also independent. This allows us to use separate models; one for the GPD

TABLE 4. Estimates and statistics of the regression coefficients for the extreme value distribution parameters. Here, λ is the threshold exceedance rate, and σ and ξ are the scale and shape parameters of the GPD. The subscript 0 (1) refers to the intercept (slope) term. The mean, standard deviation, and 95% credible interval are based on a hierarchical Bayesian specification of an extreme value model where the occurrence is governed by the threshold exceedance rate and the intensity is governed by the parameter values of the GPD. For comparison, the ML estimate (MLE) and its standard error (SE) are also provided.

Coefficient	MLE	SE	Mean	Std dev	2.5%	Median	97.5%
$\log(\lambda)_0$	−0.409	0.1130	−0.415	0.1115	−0.6402	−0.4129	−0.2031
$\log(\lambda)_1$	0.086	0.4500	0.060	0.4445	−0.8245	0.0634	0.9192
$\log(\sigma)_0$	3.229	0.1475	3.161	0.1527	2.855	3.163	3.461
$\log(\sigma)_1$	0.846	0.7023	0.864	0.7177	−0.5167	0.8520	2.299
ξ_0	−0.290	0.0937	−0.210	0.1100	−0.3964	−0.2205	0.0346
ξ_1	0.511	0.4616	0.539	0.5526	−0.5586	0.5413	1.626

parameters and another for the exceedance rate. We sample the posterior predictive storm rate and the GPD parameters, which allows us to generate sample hurricane seasons. This is a novel aspect of our methodology.

c. BUGS

The hierarchical Bayesian specification combines the prior with the GPD likelihood to generate posterior estimates for the regression coefficients of the extreme value parameters. This is accomplished using the Bayesian inference using Gibbs sampler (BUGS) software. BUGS performs Bayesian analysis of complex statistical models using Markov chain Monte Carlo (MCMC) methods (Gilks et al. 1996). We use WinBUGS (Windows version of BUGS) 1.4, which has a graphical user interface. BUGS minimizes the startup cost of Bayesian modeling by eliminating the need to program in a high-level language. It also chooses an appropriate MCMC sampling algorithm based on the model structure. The WinBUGS code used here is given as an appendix.

BUGS does not yet have support for the GPD, but it can sample from any distribution with an analytical likelihood.[3] In addition to providing the sampling distribution, we must ensure that the chosen distribution provides only probabilities between 0 and 1. We use a step function to guarantee that the probabilities are bounded below by 0 and a multiplier C to guarantee that the probabilities are bounded above by 1. Since the power function does not handle negative or zero mantissa, we use a very small value (10^{-12}) to test $1 + (\xi/\sigma) \times (y - u)$, which can be negative. Our code does not test for $\xi = 0$ as this is not a problem in sampling.

[3] The lead author is working with the BUGS community to add this support.

d. Convergence

To ensure stability of the results we run BUGS for 110 000 updates and discard the first 4000 as burn-in. Updates are successive values of the regression coefficients for the distributional parameters. In particular, we are interested in parameters of the GPD. The series of successive updates is called a Markov chain because the value of the current update depends only on the value of the previous update. The choice of how many updates to discard depends on the initial values of the chain and on the rate of converge. We test convergence by using two different sets of initial values where the intercept coefficients on the parameters are changed by 10% and calculate the modified Gelman–Rubin convergence statistic (Brooks and Gelman 1998), which is based on the ratio of the pooled 80% interval to the mean of the individual 80% intervals using moving averages from the chain. Convergence occurs when the ratio is unity. We also estimate the correlation range in the chain, which is the minimum lag at which two chains started from different initial values are uncorrelated. Values of the correlation range between 40 and 80, with the larger values associated with models having fewer wind speed estimates. Finally, we examine the chains looking for patterns in the sequence of updates that might lead one to conclude that the model had not converged. Developing more rigorous criteria for deciding chain length and burn-in goes beyond the scope of the present study.

e. Results

Table 4 summarizes the results from the Bayesian model using global temperature as the sole covariate. Values are estimates and statistics of the regression coefficients for the extreme value distributional parameters. The three distributional parameters are $\log(\lambda)$, $\log(\sigma)$, and ξ, with the regression intercept coefficient denoted with a subscript 0 [e.g., $\log(\lambda)_0$] and the regres-

sion slope coefficient denoted with a subscript 1 (e.g., ξ_1). Results are compared to an ML specification. The ML model uses data for the years 1856–2004 as global temperature data are not available before 1856. The results match quite well despite the fact that the Bayesian model includes measurement error on the hurricane wind speeds and a missing data model for the covariates.

When the global temperature anomaly is 0°C, the posterior mean logarithm of threshold exceedance rate is −0.415 using the Bayesian approach, which compares with −0.409 using the ML approach. Both methods produce a rate of 0.66 near-coastal major hurricanes per year. The positive value estimated for $\log(\lambda)_1$ indicates that warmer global temperature is conditionally associated with a greater number of major hurricanes (category 3 or higher). However, both the standard error on the ML estimate and the standard deviation from the Bayesian samples indicate that this result is not highly significant. The annual rate increases to 0.04 (0.06) major hurricanes per year for every 1° increase in global temperature according to the Bayesian (ML) model.

The positive value estimated for $\log(\sigma)_1$ indicates that warmer global temperature is associated with stronger major hurricanes, and this result is suggestive, but inconclusive as the 95% credible interval includes the value zero. Similarly, the positive value estimated for ξ_1 indicates that warmer temperature is associated with more extreme hurricane wind speeds, but the result is not statistically significant. The ξ_0 coefficient estimate is negative, indicating that the maximum near-coastal hurricane wind speed is bounded consistent with the basic heat engine theory of hurricanes that establishes an upper limit to hurricane intensity (Bister and Emanuel 1998). However, with the Bayesian model that puts a distribution on the maximum wind speed we note the ξ_0 coefficient is shifted in a positive direction with an increase in the variance on all model coefficients. The maximum possible hurricane wind speed is estimated to be 208 kt (183 kt) using the Bayesian (ML) model.

7. Summary and conclusions

Hurricanes cause significant social and economic disruption in the United States. Knowing the return periods of the most extreme winds associated with coastal hurricanes provides information for emergency planners and the insurance industry. Here we use maximum wind speed values from the HURDAT reanalysis dataset to model the return levels of extreme hurricane wind speeds near the U.S. coastline. Models from extreme value theory are used to obtain estimates of return level hurricane-force winds for return periods up to 1000 yr. Mean residual life plots are used to set the threshold wind speeds.

On average we can expect 132-kt (157 kt) hurricane winds near the U.S. coast once every 10 (100) years. Along the Florida coastline we can expect 108-kt (137 kt) winds once every 5 (50) years on average, and along the East Coast we can expect 103-kt (120 kt) hurricane winds once every 10 (500) years. The difference in model results is largest for the SOI. La Niña (El Niño) conditions are associated with a 2-yr return level of 112 (92) kt and a 500-yr return level of 141 (178) kt. The differences associated with the SOI are noted along the Gulf Coast, Florida, and the East Coast, however for the East Coast, El Niño conditions are associated with lower return levels for the longest return periods. Return level differences associated with the NAO are largest for Florida. A below- (above) average NAO 10-yr return level for Florida is 127 (112) kt.

The extreme value models derived in this paper are based on the best available hurricane data, but results need to be interpreted with caution as there are likely biases in the wind speeds, especially for hurricanes during the first half of the twentieth century. Potentially the most significant bias could be the linear interpolation used to fill in 6-h wind speeds from the once- or twice-a-day reports. For some hurricanes this will lead to an underestimation of the true wind speed near the coast and for others it will lead to an overestimation. To address this limitation, a hierarchical Bayesian approach is employed that provides a better framework for including uncertainty in the modeling process and allows the use of continuous covariates. In this limited experiment we consider the entire coast only and global temperature as the lone predictor variable. Encouragingly, the results are comparable to those from an ML approach in showing more intense hurricanes in a warmer climate.

Besides the ability to include measurement error into the analysis, the Bayesian approach is attractive for a number of reasons. The Bayesian approach provides a context in which to incorporate prior information or beliefs such as historical or proxy data into the model. This is important in light of the ongoing efforts to detect hurricane events from geological records (Liu and Fearn 1993; Donnelly et al. 2001; Scott et al. 2003) and collate historical information (Bossak and Elsner 2004).

A limitation of the methodologies discussed here is that the threshold parameter u is not estimated directly. Instead we rely on other methods to determine it. An improvement can be made by having the model estimate this parameter directly. Additional improvements

can be made by considering the regions as coastal segments (e.g., mile posts). This would require a spatial model in which the GPD parameters are allowed to vary continuously along the coast and with climate. The methodology could then be used to assign wind speed estimates to geological records. The Bayesian approach can be improved by considering an alternative prior specification that relates return levels for three different return periods (e.g., Coles and Tawn 1996).

Acknowledgments. Partial support for this study was provided by the National Science Foundation (ATM-0086958, ATM-0435628, and BCS-0213980) by the Risk Prediction Initiative (RPI-05001), and by Climatek Incorporated. The views expressed within are those of the authors and do not reflect those of the funding agencies.

APPENDIX

WinBUGS Model for Extreme Hurricane Winds

```
model
{
for(j in 1:M)
{
lsigma2[j] ← inprod(ls.x [], X[j, ])
xi2[j] ← inprod(xi.x[], X[j, ])
H[j] ~ dpois (lambda [j])
log (lambda [j]) ← inprod(tc[], X[j, ])
}
for(k in 1:Np) {
ls.x[k] ~ dnorm(0, tau.ls[k])
xi.x[k] ~ dnorm(0, tau.xi[k])
tc[k] ~ dnorm(0, tau.tc[k])
for(j in 1:M)
{
X [j, k] ~ dnorm(xmu[k], xtau [k])
}
xmu[k]~dnorm(0, 0.001)
xtau[k]~dgamma(0.01, 0.01)
}
for(i in 1:N)
{
y1[i] ← yy[i] − e[i]
ys[i] ← yy[i] + e[i]
W[i] ~ dunif(yl[i], ys[i])
yy[i] ~ dflat()
ones [i] ← 1
ones [i] ~ dbern(p[i])
offset [i] ← Yr[i] - Yr0
lsigma[i] ← lsigma2[offset [i]]
xi[i] ← xi2[offset[i]]
sigma[i] ← exp(lsigma[i])
z[i] ← (1 + xi[i]/sigma[i]*(yy[i]-u)*step(yy[i]-u))
w[i] ← max(z[i], epsilon)
p[i] ← C/(sigma[i]*pow(w[i], (1/xi[i] +1)))*step(z[i]-
   epsilon)
llik[i] ← log(p[i]/C)
}
d ← −2*sum(llik[])
maxp ← ranked (p [], N)
minp ← ranked (p [], 1)
}
```

REFERENCES

Bister, M., and K. A. Emanuel, 1998: Dissipative heating and hurricane intensity. *Meteor. Atmos. Phys.,* **50,** 233–240.

Bossak, B. H., and J. B. Elsner, 2004: Plotting early nineteenth century hurricane information. *Eos, Trans. Amer. Geophys. Union,* **85,** 1–5.

Bove, M. C., J. B. Elsner, C. W. Landsea, X. Niu, and J. J. O'Brien, 1998: Effect of El Niño on U.S. landfalling hurricanes, revisited. *Bull. Amer. Meteor. Soc.,* **79,** 2477–2482.

Brooks, S., and A. Gelman, 1998: General methods for monitoring convergence of iterative simulations. *J. Comput. Graphical Stat.,* **7,** 434–455.

Casson, E., and S. Coles, 1999: Spatial regression models for extremes. *Extremes,* **1,** 449–468.

Chan, J. C. L., and S. L. Liu, 2004: Global warming and western Pacific typhoon activity from an observational perspective. *J. Climate,* **17,** 4590–4602.

Chu, P.-S., and J. Wang, 1998: Modeling return periods of tropical cyclone intensities in the vicinity of Hawaii. *J. Appl. Meteor.,* **37,** 951–960.

Coles, S., 2001: *An Introduction to Statistical Modeling of Extreme Values.* Springer, 208 pp.

——, and J. A. Tawn, 1996: A Bayesian analysis of extreme rainfall data. *Appl. Stat.,* **45,** 463–478.

——, and L. R. Pericchi, 2003: Anticipating catastrophes through extreme value modeling. *Appl. Stat.,* **52,** 405–416.

——, ——, and S. Sisson, 2003: A fully probabilistic approach to extreme rainfall modeling. *J. Hydrol.,* **273,** 35–50.

Cressie, N. A. C., 1993: *Statistics for Spatial Data.* John Wiley and Sons, 900 pp.

Darling, R. W. R., 1991: Estimating probabilities of hurricane wind speeds using a large-scale empirical model. *J. Climate,* **4,** 1035–1046.

Donnelly, J. P., and Coauthors, 2001: A 700-year sedimentary record of intense hurricane landfalls in southern New England. *Geol. Soc. Amer. Bull.,* **113,** 714–727.

Elsner, J. B., 2003: Tracking hurricanes. *Bull. Amer. Meteor. Soc.,* **84,** 353–356.

——, and A. B. Kara, 1999: *Hurricanes of the North Atlantic: Climate and Society.* Oxford University Press, 488 pp.

——, and T. H. Jagger, 2004: A hierarchical Bayesian approach to seasonal hurricane modeling. *J. Climate,* **17,** 2813–2827.

——, and ——, 2006a: Comparison of hindcasts anticipating the 2004 Florida hurricane season. *Wea. Forecasting,* **21,** 182–192.

——, and ——, 2006b: Prediction models for annual U.S. hurricane counts. *J. Climate,* **19,** 2935–2952.

——, A. B. Kara, and M. A. Owens, 1999: Fluctuations in North Atlantic hurricanes. *J. Climate,* **12,** 427–437.

——, T. H. Jagger, and X. Niu, 2000a: Shifts in the rates of major

hurricane activity over the North Atlantic during the 20th century. *Geophys. Res. Lett.,* **27,** 1743–1746.

——, K.-B. Liu, and B. Kocher, 2000b: Spatial variations in major U.S. hurricane activity: Statistics and a physical mechanism. *J. Climate,* **13,** 2293–2305.

——, B. H. Bossak, and X.-F. Niu, 2001: Secular changes to the ENSO-U.S. hurricane relationship. *Geophys. Res. Lett.,* **28,** 4123–4126.

——, X.-F. Niu, and T. H. Jagger, 2004: Detecting shifts in hurricane rates using a Markov chain Monte Carlo approach. *J. Climate,* **17,** 2652–2666.

Emanuel, K., 1987: The dependence of hurricane intensity on climate. *Nature,* **326,** 483–485.

——, 2000: A statistical analysis of tropical cyclone intensity. *Mon. Wea. Rev.,* **128,** 1139–1152.

——, 2005: Increasing destructiveness of tropical cyclones over the past 30 years. *Nature,* **436,** 686–688.

——, S. Ravela, E. Vivant, and C. Risi, 2006: A statistical deterministic approach to hurricane risk assessment. *Bull. Amer. Meteor. Soc.,* **87,** 299–314.

Embrechts, P., C. Kliippelburg, and T. Mikosch, 1997: *Modeling Extremal Events for Insurance and Finance.* Springer, 645 pp.

Enfield, D. B., A. M. Mestas-Nunez, and P. J. Trimble, 2001: The Atlantic multidecadal oscillation and its relation to rainfall and river flows in the continental U.S. *Geophys. Res. Lett.,* **28,** 2077–2080.

Folland, C. K., and Coauthors, 2001: Global temperature change and its uncertainties since 1861. *Geophys. Res. Lett.,* **28,** 2621–2624.

Gilks, W. R., S. Richardson, and D. J. Spiegelhalter, 1996: *Markov Chain Monte Carlo in Practice.* Chapman and Hall, 486 pp.

Goldenberg, S. B., and L. J. Shapiro, 1996: Physical mechanisms for the association of El Niño and West African rainfall with Atlantic major hurricane activity. *J. Climate,* **9,** 1169–1187.

——, C. W. Landsea, A. M. Mestas-Nuñez, and W. M. Gray, 2001: The recent increase in Atlantic hurricane activity: Causes and implications. *Science,* **293,** 474–479.

Gray, W. M., 1984: Atlantic hurricane frequency: Part I: El Niño and 30 mb quasi-biennial oscillation influences. *Mon. Wea. Rev.,* **112,** 1649–1668.

Greenwood, J. A., J. M. Landwehr, and N. C. Matalas, 1979: Probability weighted moments: Definition and relation to parameters of several distributions expressible in inverse form. *Water Resour. Res.,* **15,** 1049–1054.

Heckert, N. A., E. Simiu, and T. Whalen, 1998: Estimates of hurricane wind speeds by "peaks over threshold" method. *J. Struct. Eng. ASCE,* **124,** 445–449.

Henderson-Sellers, A., and Coauthors, 1998: Tropical cyclones and global climate change: A post-IPCC assessment. *Bull. Amer. Meteor. Soc.,* **79,** 9–38.

Jagger, T. H., J. B. Elsner, and X. Niu, 2001: A dynamic probability model of hurricane winds in coastal counties of the United States. *J. Appl. Meteor.,* **40,** 853–863.

Jarvinen, B. R., C. J. Neumann, and M. A. S. Davis, 1984: A tropical cyclone data tape for the North Atlantic Basin, 1886–1983: Contents, limitations, and uses. NOAA Tech. Memo. NWS NHC-22, Coral Gables, FL, 21 pp.

Jones, P. D., T. Jónsson, and D. Wheeler, 1997: Extension to the North Atlantic Oscillation using early instrumental pressure observations from Gibraltar and South–West Iceland. *Int. J. Climatol.,* **17,** 1433–1450.

Katz, R. W., M. B. Parlange, and P. Naveau, 2002: Statistics of extremes in hydrology. *Adv. Water Resour.,* **25,** 1287–1304.

Knutson, T. R., and R. E. Tuleya, 2004: Impact of CO_2-induced warming on simulated hurricane intensity and precipitation: Sensitivity to the choice of climate model and convective parameterization. *J. Climate,* **17,** 3477–3495.

Landsea, C. W., R. A. Pielke Jr., A. M. Mestas-Nuñez, and J. A. Knaff, 1999: Atlantic basin hurricanes: Indices of climatic changes. *Climate Change,* **42,** 89–129.

——, and Coauthors, 2004: The Atlantic hurricane database reanalysis project: Documentation for 1851–1910: Alterations and additions to the HURDAT database. *Hurricanes and Typhoons: Past, Present, and Future,* R. J. Murnane and K.-B. Liu, Eds., Columbia University Press, 177–221.

Lighthill, J., and Coauthors, 1994: Global climate change and tropical cyclones. *Bull. Amer. Meteor. Soc.,* **75,** 2147–2157.

Liu, K.-B., and M. L. Fearn, 1993: Lake-sediment record of late Holocene hurricane activities from coastal Alabama. *Geology,* **21,** 793–796.

McNeil, A. J., and T. Saladin, 2000: Developing scenarios for future extreme losses using the POT method. *Extremes and Integrated Risk Management,* P. M. E. Embrechts, Ed., RISK Books, 253–275.

Murnane, R. J., and Coauthors, 2000: Model estimates hurricane wind speed probabilities. *Eos, Trans. Amer. Geophys. Union,* **81,** 433–438.

Neumann, C. J., B. R. Jarvinen, C. J. McAdie, and G. R. Hammer, 1999: *Tropical Cyclones of the North Atlantic Ocean, 1871–1998.* National Oceanic and Atmospheric Administration, 206 pp.

Palutikof, J. P., B. B. Brabson, D. H. Lister, and S. T. Adcock, 1999: A review of methods to calculate extreme wind speeds. *Meteor. Appl.,* **6,** 119–132.

Pang, W.-K., J. J. Forster, and M. D. Troutt, 2001: Estimation of wind speed distribution using Markov chain Monte Carlo techniques. *J. Appl. Meteor.,* **40,** 1476–1484.

Pielke, R. A., Jr., C. Landsea, M. Mayfield, J. Laver, and R. Pasch, 2005: Hurricanes and global warming. *Bull. Amer. Meteor. Soc.,* **86,** 1571–1575.

Ropelewski, C. F., and P. D. Jones, 1987: An extension of the Tahiti–Darwin Southern Oscillation Index. *Mon. Wea. Rev.,* **115,** 2161–2165.

Rupp, J. A., and M. A. Lander, 1996: A technique for estimating recurrence intervals of tropical cyclone–related high winds in the Tropics: Results for Guam. *J. Appl. Meteor.,* **35,** 627–637.

Scott, D. B., E. S. Collins, P. T. Gayes, and E. Wright, 2003: Records of prehistoric hurricanes on the South Carolina coast based on micropaleontological and sedimentological evidence, with comparison to other Atlantic Coast records. *Geol. Soc. Amer. Bull.,* **115,** 1027–1039.

Walshaw, D., 2000: Modelling extreme wind speeds in regions prone to hurricanes. *Appl. Stat.,* **49,** 51–62.

Webster, P. J., G. J. Holland, J. A. Curry, and H.-R. Chang, 2005: Changes in tropical cyclone number, duration, and intensity in a warming environment. *Science,* **309,** 1844–1846.